Freezing of polydisperse hard spheres

David A. Kofke
Department of Chemical Engineering, State University of New York at Buffalo, Buffalo, New York 14260-4200

Peter G. Bolhuis
Department of Chemistry, University of California at Berkeley, Berkeley, California 94720

(Received 13 March 1998; revised manuscript received 19 August 1998)

Freezing of polydisperse hard spheres is studied by Monte Carlo simulation and the results are interpreted with a cell model of the solid. The results supplement an earlier study of freezing of nearly monodisperse hard spheres and, within the assumption of a substitutionally disordered solid, a complete description of the freezing behavior is obtained. The density and polydispersity of the precipitate are characterized by a single curve, regardless of the composition of the fluid from which it is formed. Fractionation enables a fluid of arbitrary polydispersity to precipitate a solid of small polydispersity, dispeling the long-held notion of a fluid-phase ''critical'' polydispersity, beyond which it cannot form a solid. Nevertheless, a primary conclusion from the previous study is confirmed: a solid crystalline phase of polydispersity exceeding 5.7% of the average sphere diameter cannot be precipitated from a fluid phase. [S1063-651X(98)04312-8]

PACS number(s): 64.70.Dv, 61.20.Ja, 64.60.Cn, 82.70.Dd

The freezing transition of a system of pure hard spheres was demonstrated by some of the earliest molecular simulations [1], and the precise location of the transition was later determined by free-energy calculations [2]. The hard-sphere model provides a crude but reasonable description of the behavior of some colloidal systems [3], and an ordering transition that has been observed in uncharged monodisperse colloids is consistent with the hard-sphere behavior [4,5]. Real colloidal systems often comprise spheres of varying size, and the effect of this polydispersity on the ordering behavior is not well understood. The influence of polydispersity has been examined with theory [6], molecular simulation [7,8], and experiment [5]. A general conclusion from all of these studies is the existence of an upper limit on size polydispersity, a ''terminal polydispersity'' above which no crystallization can occur. If the polydispersity is defined as the standard deviation of the size distribution divided by the mean, then the various studies indicate that the terminal polydispersity is in the range of 5–15 %. Almost all studies based in theory or molecular simulation invoke some assumption regarding the distribution of particle diameters between the two phases, typically taking them to be identical. In principle, this approach is incorrect, as phase equilibria in mixtures generally involve some fractionation, with components of the mixture distributing themselves unevenly between the phases. This ''constrained eutectic'' approximation is reasonable only for small polydispersity.

We recently reported [8] a molecular simulation study of the freezing transition of polydisperse hard spheres. These simulations were conducted in a semigrand ensemble [9,10] and employed the Gibbs-Duhem integration (GDI) technique [10,11] to follow the coexistence behavior as a function of size polydispersity. The study provided an essentially exact description of the freezing transition, and it found that fractionation begins to show at a polydispersity of approximately 3%. The study also indicated the existence of a terminal polydispersity which, due to fractionation, is different in the solid and fluid phases: 5.7 and 11.8 %, respectively.

It is important to understand how the terminus arises in the simulation study. In the semigrand ensemble an independent variable is the distribution of chemical potential differences $\Delta\mu(\sigma)$, or activity ratios $a(\sigma)=\exp(\Delta\mu(\sigma))$, where σ is the hard-sphere diameter (to simplify notation we take unit temperature kT). This distribution is imposed on both phases, thereby ensuring equality of all species chemical potentials as long as the chemical potential of an arbitrary reference species is made equal in the two phases. This requirement is met by the GDI procedure via selection of an appropriate value of the coexistence pressure (also imposed on both phases). The imposed activity distribution is Gaussian with variance ν, which thereby becomes the variable used to control the polydispersity. The GDI method traces the locus of states in the (P,ν) plane for which the solid and fluid are in equilibrium. The initial condition for the integration is the monodisperse limit, $\nu\to 0$, at which the coexistence pressure is known. Integration proceeds in a direction of increasing ν. As the activity distribution becomes less sharp, the mixtures become increasingly nonideal, and the composition distribution migrates away from the imposed activity distribution. The shift in both phases is toward smaller diameters.

Eventually the integration path bends back, and the coexistence pressure grows without bound as the parameter ν returns to zero. The resulting distribution of diameters is such that most spheres are vanishingly small. Nevertheless, physically relevant results can be recovered by scaling all quantities by a mean diameter. In particular upon rescaling it is found that the polydispersity continues to increase (despite the decrease in ν) and the pressure remains finite. As this regime takes hold, the interpretation of ν as a measure of polydispersity becomes inappropriate. The diameter distribution is highly skewed away from the imposed Gaussian activity, and is so narrow that the chemical potential distribution is essentially linear across it. Here, ν can be interpreted only as (the reciprocal of) the slope of this linear distribution. The system is analogous to one in which Hookean springs

attempt to push the spheres to larger diameters, while the external pressure constrains them to finite values. The single state parameter for this limiting system is the ratio of the pressure to this ''spring constant.'' Only one value of this ratio is consistent with solid-fluid coexistence (just as only one pressure is possible for coexisting solid and fluid monodisperse hard spheres); hence when the limit is reached no further variation is possible and the coexistence line terminates.

In this paper, we extend this integration procedure from the previously identified terminus by imposing a chemical-potential distribution containing quadratic or cubic terms in the sphere diameter. Interestingly, this process finds that the saturated solid phase becomes increasingly monodisperse and close-packed while the saturated fluid adopts increasingly large polydispersity, i.e., fractionation increases. The narrowness of the solid-phase diameter distribution permits its chemical potentials to be well characterized by a linear form, so the higher-order terms in the chemical-potential distribution have their greatest effect on the fluid phase only. This outcome imbues the study with a generality we discuss below.

Before continuing, it is worth remembering the notion of equivalence of ensembles [12], which permits us to study polydisperse hard spheres as though the diameters were fluctuating under the influence of ''internal springs'' and still draw conclusions about the coexistence behavior of real colloidal spheres each of fixed diameter. The device of fluctuating the diameters facilitates the phase-coexistence calculation, and should be viewed as the sampling of different physical regions of the solid and fluid; for this analysis to be valid it is by no means necessary that the spheres in the real system actually fluctuate in diameter.

We conduct our Monte Carlo (MC) simulations in the isobaric semigrand ensemble, for which the distribution of chemical potential differences $\Delta\mu$ is an independent (functional) parameter. We are interested in including terms up to cubic in the sphere diameter σ

$$\Delta\mu(\sigma)=c_1\sigma+c_2\sigma^2+c_3\sigma^3. \tag{1}$$

The identity of the ''reference'' diameter, against which the difference is formed, is not important and for convenience we take it to be zero. The c_1 terminus identified in [8] corresponds to $c_1=1$ with $c_2=c_3=0$ (here c_1 sets the length scale). To depart from this point we apply the GDI method [10,11] to follow the coexistence line as c_2 or c_3 is increased from zero. The governing Clapeyron-like equation is

$$\frac{dP}{dc_k}=\frac{\Delta s_k}{\Delta v}, \tag{2}$$

where s_k is the kth moment (about the origin) of the diameter distribution, v is the volume per molecule, and the Δ indicates a difference between the two coexisting phases. Both quantities are measured by the MC simulation, and a predictor-corrector procedure is applied to integrate this differential equation, as described elsewhere [8,10,11].

The volume integral in the isobaric ensemble average can be evaluated analytically, so MC sampling of the volume is not necessary [8]. A closely connected result is an exact scaling formula that relates the pressure to the moments of the composition distribution [13]. For the $\Delta\mu$ distribution of Eq. (1), this relation is

$$3(P/\rho-1)=1+c_1s_1+2c_2s_2+3c_3s_3, \tag{3}$$

where $\rho=1/v$ is the number density. In the semigrand ensemble the moments are not known *a priori* so this formula is not a self-contained equation of state, but it is useful nonetheless.

Several integration series were performed, differing in the choice of integration path and the method for characterizing the fluid phase. In some series simulation was used to characterize both phases. In other series we applied the hard-sphere mixture equation of Mansoori *et al.* [14] (MCSL) in lieu of simulation of the fluid. We used the fluid-phase equation of state because we were concerned about the ability of the fluid-phase simulations to converge at high pressure. Of course, the validity of the equation of state may be questioned in this regime too. Simulations of the solid and fluid phases were performed with system sizes of 256 or 864 particles in each phase. In each simulation 20 000 simulation cycles were performed, where one simulation cycle comprises one translation attempt and one diameter-change trial per particle (on average; trial particles were always selected at random).

Two series were performed from the c_1 terminus. In one the c_2 coefficient was increased from zero with c_1 fixed at unity (thereby setting the length scale); in another series the c_3 coefficient was instead increased. The c_2 series terminated naturally (with $c_2/c_1^2\to\infty$) much as the original series [8] did. At this new terminus a second ''c_3 series'' was initiated, using the MCSL equation for the fluid phase. Both c_3 series were extended to the point where the approach broke down, either because the MCSL equation of state had no solution for the given $\Delta\mu$ distribution, or because the simulations were extremely sluggish at converging (owing to the high density of the simulated fluid).

In Fig. 1 results are presented in the volume fraction-polydispersity plane. The original c_1 terminus and the new c_2 terminus are indicated. Several tie lines joining coexisting fluid and solid phases are presented as well. Two features are notable. First, the fluid-phase curves differ with the choice of integration path (i.e., whether c_2 is integrated before initiating the c_3 integration). This, of course, is not a surprising outcome. The coexistence density and polydispersity should be expected to depend on details of the imposed chemical potential distribution. Therefore, it is surprising that a corresponding difference is not observed in the coexisting solid. All solid-phase coexistence curves are practically indistinguishable. The second feature worth noting is the behavior of this ''universal'' solid-phase curve. In all cases the integration proceeds to a solid that becomes increasingly monodisperse and increasingly dense, approaching a pure, closed-packed solid phase. This limiting solid is in equilibrium with a highly polydisperse fluid. It must be emphasized that before this limit is reached it is likely that the fluid-phase data becomes compromised, perhaps by the onset of a glass transition, and almost certainly by limits of the convergence rate of the simulation; thus at some point the fluid-phase data must be viewed only qualitatively.

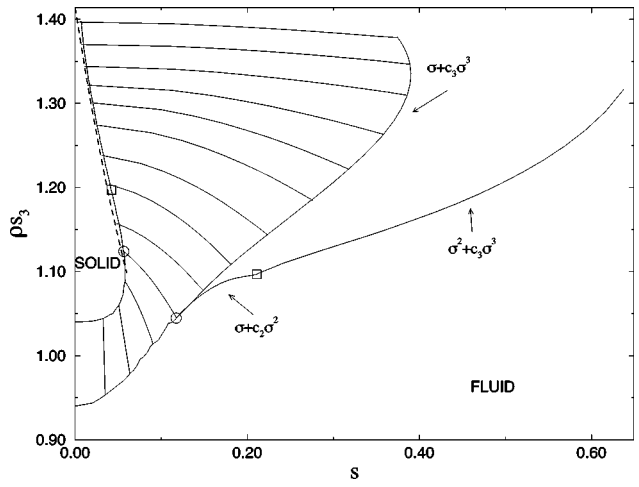

FIG. 1. Coexisting fluid and solid phases in the volume fraction (ρs_3)—polydispersity plane. Tie lines connect a few coexisting phases. Both the $c1$ (open circles) and the c_2 terminus (squares) are shown. The labels at the fluid lines refer to the form of the chemical potential difference used in the GDI integration. The dashed line is the description of the solid phase according to the cell model.

The approach to monodisperse close packing is interesting, especially in light of the finding that such a system can be precipitated from a fluid phase. The narrowness of the composition distribution permits us to treat the imposed chemical potential distribution as a linear form [only c_1 nonzero in Eq. (1)]. The need to apply a cubic distribution to reach this limit has more to do with the behavior of the coexisting fluid than with the solid. Accordingly, we consider a simple cell-model description of the limit of close packing for the linear case.

Cottin and Monson have made a lot of progress recently in applying canonical-ensemble cell models to understand the freezing behavior of hard-sphere mixtures [15]. We instead work in the semigrand ensemble. In addition, we exploit some simplifications that accompany the approach to close packing to develop analytical relations for the thermodynamic properties. In this regard this treatment for mixtures is an extension of the methods used to model the approach of monodisperse hard spheres to their close-packing limit [16]. We see the semigrand ensemble as providing the only viable framework to conduct this high-density analysis for polydisperse mixtures.

The (constant volume) semigrand-canonical ensemble [9,10] partition function Υ for an uncorrelated cell model is written as the product of cell partition functions: $\Upsilon=\upsilon^N$. The single-cell partition function υ integrates over all positions and diameters of a hard sphere within the unit cell. The positions are constrained by the requirement of no overlap with spheres in neighboring cells, which are fixed at their lattice positions and which are of fixed diameter s_1; the diameter s_1 will be determined self-consistently in the treatment. For a given diameter of the central sphere, the integral over positions is well approximated by the volume of an appropriate dodecahedron (assuming the solid forms an fcc lattice), in which case the unit-cell partition function is

$$\upsilon=\frac{V_D}{\Lambda^3\sigma_0}\int_0^{\sigma_{\max}} e^{c_1\sigma}\left[\sigma_{cp}-\frac{1}{2}(\sigma+s_1)\right]^3 d\sigma, \tag{4}$$

TABLE I. Coefficients describing the composition moments, as determined by the cell model and by MC simulation (extrapolated to infinite system size). Numbers in parentheses indicate the confidence limits of the last digit of the value.

	q_1	q_2	q_3
Cell model	4	4	−8
Simulation	4.0001(2)	6.547(2)	−7.80(4)

where $\sigma_{cp}=(\sqrt{2}/\rho)^{1/3}$ is the nearest-neighbor separation for a lattice of density ρ, and $\sigma_{\max}=2\sigma_{cp}-s_1$ is the maximum diameter without overlap; also $V_D=4\sqrt{2}$ is the volume of a rhombic dodecahedron for which an inscribed sphere has unit radius; σ_0 is a unit diameter that serves only to make the partition function dimensionless [17], and Λ is the thermal wavelength.

In the close-packing limit the slope c_1 becomes infinite, and the average diameter s_1 approaches σ_{cp}. It is appropriate to express s_1 as a series in $1/c_1$: $s_1=\sigma_{cp}-q_1/c_1+O(1/c_1^2)$, with the coefficient q_1 to be determined by the analysis. The integral in Eq. (4) is easily evaluated and yields for the cell-model free energy per particle $y=-\ln\upsilon$

$$y=-\ln\frac{3V_D}{4\Lambda^3\sigma_0}+4\ln c_1-c_1\sigma_{cp}-q_1. \tag{5}$$

The first moment of the composition distribution is given by the derivative $\partial y/\partial c_1$; setting this equal to s_1 produces the result $q_1=4$. Within the uncorrelated cell model approximation the higher moments can be obtained by further differentiation with respect to c_1. In summary, to lowest order in $1/c_1$,

$$s_1=\sigma_{cp}-q_1/c_1, \tag{6}$$

$$m_2=q_2/c_1^2, \tag{7}$$

$$m_3=q_3/c_1^3, \tag{8}$$

with m_k as the kth moment about the mean s_1. The dimensionless cell-model coefficients q_k are recorded in Table I. The equation of state is obtained most easily (and with no further approximation) via the scaling relation, Eq. (3). The chemical potential $\mu(\sigma)$ of a sphere of diameter σ is then obtained from its relation to the semigrand free energy and the pressure:

$$\mu(\sigma)=y+P/\rho+\Delta\mu(\sigma). \tag{9}$$

We performed semigrand-ensemble MC simulations of a single phase of nearly close-packed polydisperse hard spheres for $\rho^{1/3}c_1$ ranging from 10^4 to 10^7, examining the system-size dependence to extrapolate to infinite size. The simulations confirm the scaling with c_1 indicated by the cell model. However, the simulations find that the coefficients of the scaling relations are incorrect for the second and third moments. Results are presented in Table I. Not surprisingly, the cell-model second moment is too small because the treatment ignores fluctuations in the diameters of the neighbors of the central sphere, fluctuations which can only cause the dis-

tribution of diameters to become wider than the uncorrelated prediction. We made several attempts to develop correlated models but did not find satisfactory improvement. MC simulations of cell models of varying degree of approximation indicate that many-neighbor correlations are needed to yield any improvement in the higher moments.

Elimination of c_1 between the moments in Eqs. (6)–(8) permits comparison with the MC density-polydispersity phase diagram. The corresponding cell-model curve is presented as a dashed line in Fig. 1. This curve was computed according to the c_1-scaling relations prescribed by the cell model, but with corrected values of the coefficients recorded in Table I. We must emphasize that the linear chemical potential approach, and the cell model based upon it, applies only to a precipitating solid; it is not valid as a general equation of state for a polydisperse solid away from coexistence.

The complete solid-fluid coexistence diagram for polydisperse hard spheres exhibits two regions in which the solid phase is nearly monodisperse. The first is the region that was used to initiate this study in our previous work [8]. Here, the solid is monodisperse because the fluid is too; i.e., it is monodisperse because all spheres in the complete fluid-solid system are of nearly the same diameter. This case is marked by an equally narrow activity distribution. The other nearly-monodisperse coexisting solid does not have a narrow activity distribution. Instead the distribution increases exponentially over the (narrow) range of diameters. Consequently, this phase can be equilibrated with a lower-density fluid phase of arbitrarily large polydispersity. *The details of the activity distribution beyond the narrow range of diameters are of no consequence to the solid phase.* Thus, such a solid can be precipitated from any polydisperse hard-sphere fluid; the principal limitation is whether the fluid can be sufficiently compressed without forming a glass. Nevertheless our previous conclusion [8] regarding the terminal polydispersity of the solid phase remains: a stable, substitutionally disordered crystalline phase of polydispersity exceeding 5.7% of the average sphere diameter cannot be formed from a fluid phase.

One can apply a fluid-phase model (e.g., the MCSL equation of state [14]) in conjunction with the cell model outlined above to predict the existence and nature of a substitutionally disordered solid precipitate for an arbitrary polydisperse hard-sphere fluid phase. Given a fluid phase of known composition at a pressure P, one could proceed as follows:

(i) Guess a value s_1 of the average diameter of the solid precipitate. (ii) Using the model of the fluid phase, compute the local slope c_1 of the fluid-phase chemical-potential distribution at the diameter s_1. (iii) Within the approximation of the cell model a solid phase corresponding to these values of P, c_1, and s_1 can exist only if a density can be found satisfying both Eqs. (3) and (6). This requires (taking $q_1=4$)

$$Ps_1^3=\frac{\sqrt{2}}{3}\frac{(c_1s_1)^3}{(c_1s_1+4)^2}. \tag{10}$$

(iv) If Eq. (10) is obeyed for some s_1, then the solid phase will precipitate from the fluid if the candidate fraction has a lower chemical potential in the solid. This outcome can be tested by comparing the chemical potential at $\sigma=s_1$ from the fluid model to the cell model value of Eq. (9).

One might then find that a solid is precipitated continuously as the pressure is increased, forming crystalline domains of different average diameter. Alternatively the solid might form a single quasicrystalline phase with sphere diameters that vary continuously with position. A related issue is the formation of quasicompounds—crystals that exhibit long-range ordering of the average sphere diameters. Two-component hard-sphere mixtures are known to form stable compounds of the type AB, AB_2, and AB_{13} [18]. However, these crystals arise only for spheres differing greatly in size (size ratios on the order of 0.6); in the present work the observed upper bound of $\sim 6\%$ polydispersity corresponds to a smallest-sphere/largest-sphere size ratio barely below 0.9. Moreover, the systems simulated in this work had the freedom to adopt bimodal distributions and form compounds, but this behavior was not observed. Nevertheless, it seems likely that substitutionally ordered phases are part of the overall freezing behavior of polydisperse hard spheres, and may be relevant to the freezing of highly polydisperse fluid phases.

This work was supported by the U.S. Department of Energy, Office of Basic Energy Sciences under Contract No. DE-FG02-96ER14677.

[1] B. J. Alder and T. E. Wainwright, J. Chem. Phys. **27**, 1208 (1957); W. W. Wood and J. D. Jacobson, *ibid.* **27**, 1207 (1957).

[2] W. G. Hoover and F. H. Ree, J. Chem. Phys. **49**, 3609 (1968); D. Frenkel and A. J. C. Ladd, *ibid.* **81**, 3188 (1984).

[3] W. B. Russel, D. A. Saville, and W. R. Schowalter, *Colloidal Dispersions* (Cambridge University Press, Cambridge, 1989).

[4] S. Hachisu and Y. Kobayashi, J. Colloid Interface Sci. **46**, 470 (1974); C. G. de Kruif, J. W. Jansen, and A. Vrij, in *Complex and Supramolecular Fluids*, edited by S. A. Safran and N. A. Clark (Wiley Interscience, New York, 1987).

[5] P. Pusey, in *Les Houches, sesion LI, Liquids, Freezing and Glass Transitions*, Nato ASI, edited by J.P. Hansen, D. Jevesque, and J. Zinn-Justin (North-Holland, Amsterdam, 1991).

[6] P. Pusey, J. Phys. (Paris) **48**, 709 (1987); J. L. Barrat and J.-P. Hansen, *ibid.* **46**, 1547 (1986); R. McRae and A. D. J. Haymet, J. Chem. Phys. **88**, 1114 (1988).

[7] E. Dickinson, Faraday Discuss. Chem. Soc. **65**, 127 (1978); E. Dickinson, R. Parker, and M. Lal, Chem. Phys. Lett. **79**, 578 (1981); E. Dickinson and R. Parker, J. Phys. (France) Lett. **46**, L229 (1985).

[8] P. Bolhuis and D. A. Kofke, Phys. Rev. E **54**, 634 (1996).

[9] R. B. Griffiths and J. C. Wheeler, Phys. Rev. A **2**, 1047 (1970); J. G. Briano and E. D. Glandt, J. Chem. Phys. **80**, 3336 (1984); D. A. Kofke and E. D. Glandt, *ibid.* **87**, 4881 (1987).

[10] D. A. Kofke, Adv. Chem. Phys. **105**, 405 (1998).
[11] D. A. Kofke, J. Chem. Phys. **98**, 4149 (1993).
[12] D. A. McQuarrie, *Statistical Mechanics* (Harper & Row, New York, 1976).
[13] D. A. Kofke and E. D. Glandt, J. Chem. Phys. **90**, 439 (1989).
[14] G. A. Mansoori, N. F. Carnahan, K. E. Starling, and T. W. Leland, Jr., J. Chem. Phys. **54**, 1523 (1971).
[15] X. Cottin and P. A. Monson, J. Chem. Phys. **102**, 3354 (1995); **99**, 8914 (1993).
[16] B.J. Alder, W.G. Hoover, and D.A. Young, J. Chem. Phys. **49**, 3688 (1968).
[17] The unit diameter σ_0 could be avoided by working with a dimensionless species-identifying parameter rather than using the hard-sphere diameter directly. Such an approach complicates the notation and presentation to a degree that we prefer to avoid here.
[18] M. D. Eldridge, P. A. Madden, and D. Frenkel, Nature (London) **365**, 35 (1993).